IRis

Northeastern University

Physics Faculty Publications

Department of Physics

December 28, 2006

Systematic doping evolution of the underlying Fermi surface of $La_{2-x}Sr_xCuO_4$

T. Yoshida
University of Tokyo

X. J. Zhou
Stanford University

K. Tanaka
University of Tokyo

W. L. Yang
Stanford University

Z. Hussain
Lawrence Berkeley National Laboratory

See next page for additional authors

Recommended Citation

Yoshida, T.; Zhou, X. J.; Tanaka, K.; Yang, W. L.; Hussain, Z.; Shen, Z. X.; Fujimori, A.; Sahrakorpi, S.; Lindroos, M.; Markiewicz, R. S.; Bansil, A.; Komiya, Seiki; Ando, Yoichi; Eisaki, H.; Kakeshita, T.; and Uchida, S., "Systematic doping evolution of the underlying Fermi surface of $La_{2-x}Sr_xCuO_4$" (2006). *Physics Faculty Publications.* Paper 433.

This work is available open access, hosted by Northeastern University.

Author(s)
T. Yoshida, X. J. Zhou, K. Tanaka, W. L. Yang, Z. Hussain, Z. X. Shen, A. Fujimori, S. Sahrakorpi, M. Lindroos, R. S. Markiewicz, A. Bansil, Seiki Komiya, Yoichi Ando, H. Eisaki, T. Kakeshita, and S. Uchida

This article is available at IRis: http://iris.lib.neu.edu/physics_fac_pubs/433

Systematic doping evolution of the underlying Fermi surface of $La_{2-x}Sr_xCuO_4$

T. Yoshida,[1,2] X. J. Zhou,[2] K. Tanaka,[1] W. L. Yang,[2] Z. Hussain,[3] Z.-X. Shen,[2] A. Fujimori,[1] S. Sahrakorpi,[4] M. Lindroos,[4,5] R. S. Markiewicz,[4] A. Bansil,[4] Seiki Komiya,[6] Yoichi Ando,[6] H. Eisaki,[7] T. Kakeshita,[8] and S. Uchida[9]

[1]*Department of Complexity Science and Engineering, University of Tokyo, Kashiwa, Chiba 277-8561, Japan*
[2]*Department of Applied Physics and Stanford Synchrotron Radiation Laboratory, Stanford University, Stanford, California 94305, USA*
[3]*Advanced Light Source, Lawrence Berkeley National Lab, Berkeley, California 94720, USA*
[4]*Physics Department, Northeastern University, Boston, Massachusetts 02115, USA*
[5]*Institute of Physics, Tampere University of Technology, P.O. Box 692, 33101 Tampere, Finland*
[6]*Central Research Institute of Electric Power Industry, Komae, Tokyo 201-8511, Japan*
[7]*National Institute of Advanced Industrial Science and Technology, Tsukuba 305-8568, Japan*
[8]*Superconductivity Research Laboratory, ISTEC, Shinonome 1-10-13, Koto-ku, Tokyo 135-0062, Japan*
[9]*Department of Physics, University of Tokyo, Bunkyo-ku, Tokyo 113-0033, Japan*

(Received 23 October 2005; revised manuscript received 8 November 2006; published 28 December 2006)

We have performed a systematic doping-dependent study of $La_{2-x}Sr_xCuO_4$ (LSCO) ($0.03 \leqslant x \leqslant 0.3$) by angle-resolved photoemission spectroscopy. Over this entire doping range, the underlying "Fermi surface" determined from the low-energy spectral weight approximately satisfies Luttinger's theorem, even down to the lightly doped region. This is in strong contrast to the results on $Ca_{2-x}Na_xCuO_2Cl_2$ (Na-CCOC), which show a clear deviation from Luttinger's theorem. We correlate these differences between LSCO and Na-CCOC with differences in the behavior of chemical potential shift and spectral weight transfer induced by hole doping.

DOI: 10.1103/PhysRevB.74.224510 PACS number(s): 74.25.Jb, 71.18.+y, 74.72.Dn, 79.60.−i

I. INTRODUCTION

The pseudogap behaviors in the underdoped high-T_c cuprates have attracted significant attention and have been one of the most challenging problems in strongly correlated systems. The opening of the pseudogap around $k=(\pi,0)$, which has been observed by angle-resolved photoemission spectroscopy (ARPES) studies,[1] causes electronic specific heat γ (Refs. 2–4) and Pauli paramagnetic susceptibil χ_s (Ref. 4) to decrease with decreasing hole concentration x. This unconventional behavior in the underdoped cuprates is thought to provide a remarkable example of a strong deviation from the normal Fermi-liquid picture. However, it is unclear if this behavior can be understood starting from a Fermi liquid or if its explanation requires a fundamentally new kind of ground state.[5,6]

Insofar as the Fermi surface is concerned, two radically different pictures in the underdoped cuprates have been discussed—namely, a large Fermi surface centered at (π,π) or a small Fermi surface centered at $(\pi/2,\pi/2)$. In theories starting from the Fermi liquid influenced by strong antiferromagnetic fluctuations, a large Fermi surface has been obtained.[7] Uniform resonant-valence-bond (RVB) states,[8] cellular dynamical mean-field theory (CDMFT),[9] etc., also basically lead to a large Fermi surface. On the other hand, the flux RVB and other kinds of exotic symmetry breaking[5,6] lead to a small Fermi surface. In the Fermi-liquid theory, the carrier number is given by the Fermi-surface volume (Luttinger's theorem). However, even for a large Fermi surface, numerical calculations on the Hubbard and t-J models have predicted noticeable deviation from Luttinger's theorem in the underdoped region in that the occupied area of the Fermi surface becomes significantly larger than that expected from the hole count.[10–12]. Since Luttinger's theorem lies at the heart of the Fermi-liquid concept, systematic experimental studies of the Fermi surface and its volume changes as a function of hole doping are crucial for understanding the pseudogapped state.

Recent ARPES studies on lightly doped cuprates[13,14] have shown that the Fermi surface is basically large and that, while the $(\pi,0)$ region remains (pseudo)gapped, a quasiparticle (QP) band which crosses the Fermi level (E_F) in the nodal $(0,0)$-(π,π) direction is formed, leading to the notion that only part of the Fermi surface survives as an "arc" around the node. The QP crossing in the lightly doped $La_{2-x}Sr_xCuO_4$ (LSCO) (Ref. 13) and $Ca_{2-x}Na_xCuO_2Cl_2$ (Na-CCOC) (Ref. 15) is certainly responsible for the metallic behavior.[16] The volume of the "Fermi surface" in Na-CCOC (defined under this Fermi-arc–pseudogap scenario) was found to deviate from Luttinger's theorem as doping approaches zero,[14] consistent with theoretical predictions.[10–12,17,18]

In the present paper, the evolution of the unconventional electronic structure of LSCO in the presence of Fermi arcs and pseudogap are investigated systematically via ARPES over a wide doping range. We delineate how the "Fermi surface" evolves with hole doping and find that, in sharp contrast to the case of Na-CCOC,[14] the Fermi surface area almost satisfies Luttinger's theorem even down to $x \sim 0.03$—namely, down to the "spin-glass" region. We comment on possible phenomenological and microscopic origins of the differences between the two systems.

II. EXPERIMENT

The ARPES measurements were carried out at BL10.0.1 of Advanced Light Source, using incident photons of 55.5 eV. We used a SCIENTA SES-2002 analyzer with total energy resolution of 20 meV and momentum resolution of $0.02\pi/a$, where $a=3.8$ Å is the lattice constant. High-quality

 ©2006 The American Physical Society

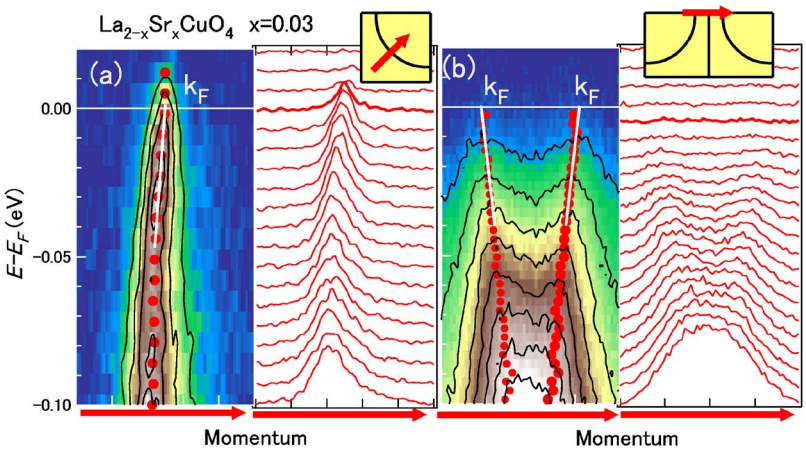

FIG. 1. (Color online) ARPES spectra of $La_{1.97}Sr_{0.03}CuO_4$. (a) Intensity plot in E-k space (left) and MDC's (right) for the nodal cut (inset). (b) Intensity plot in E-k space (left) and MDC's (right) for the antinodal cut near $(\pi,0)$ (inset). Red dots give peak positions in MDC's. Even in the pseudogap region near $(\pi,0)$, one can determine k_F by extrapolating the MDC peaks to E_F.

single crystals of LSCO were grown by the traveling-solvent floating-zone method. The critical temperatures (T_c) for the $x=0.07$, 0.15, and 0.22 samples were 14, 41, and 22 K, respectively, and the $x=0.03$ and 0.30 samples were nonsuperconducting. The samples were cleaved *in situ* and measurements were performed at 20 K as in our previous studies.[20] In the present measurements, the electric field vector **E** of the incident photons lies in the CuO_2 plane, rotated by 45° from the Cu-O bond direction, so that its direction is parallel to the Fermi-surface segment around the nodal region. This measurement geometry enhances dipole matrix elements in this **k** region.[20]

III. RESULTS AND DISCUSSION

A. Underlying Fermi surface and energy dispersion

Figure 1 shows ARPES data for LSCO ($x=0.03$), illustrating how the "Fermi-surface crossing" in the pseudogapped state can be determined from the momentum distribution curves (MDC's). In the nodal direction [(a)], where there is no gap, the underlying Fermi surface is easily determined by the MDC peak position at E_F. Near the $(\pi,0)$ point [(b)], on the other hand, the spectral weight is strongly suppressed due to pseudogap formation. However, as shown in panel (b), one can determine k_F by extrapolating MDC peaks to the E_F, even when the spectral weight is suppressed in going towards E_F. Hereafter, we refer to the Fermi surface thus determined in the pseudogapped state as the "underlying" Fermi surface.

Accordingly, we have determined the (underlying) Fermi surfaces for the entire doping range from the intensity maps shown in Fig. 2. Here, red dots indicate the k_F values determined by using MDC's as described above. From the k_F points in the first and second Brillouin zones (BZ's) and the shadow band in the first BZ,[21] we could precisely determine the absolute position of the Fermi surface at all doping levels considered. While the optimal and overdoped samples ($x \geqslant 0.15$) show strong intensities over the entire Fermi surface, the underdoped samples ($x \leqslant 0.1$) display weak or suppressed spectral weight around $(\pi,0)$—i.e., a "truncated" Fermi surface or a Fermi "arc" due to the pseudogap formation around $(\pi,0)$.

The intensity plots in E-k space of Fig. 3 clearly show how the intensity at E_F around $(\pi,0)$ becomes weak for $x \leqslant 0.15$ as the pseudogap and/or superconducting gap open up around $(\pi,0)$. On the other hand, no pseudogap behaviors were observed, in the overdoped $x=0.22$ and 0.30 samples. The width of the energy distribution curves (EDC's) becomes sharper and a clear QP feature crosses the E_F on the $(0,0)$-$(\pi,0)$ cut in this doping range. The crossover from the pseudogap state in $x=0.15$ to the Fermi-liquid-like metal in $x=0.22$ seems to be related to the topological change of the Fermi surface from a holelike to an electronlike Fermi surface. Therefore, we infer that the topological change of the Fermi surface has a significant affect on the appearance of the pseudogap. Also, the present results indicate that the QP density of states is enhanced between $x=0.15$ and 0.22 because the flatband around $(\pi,0)$ crosses the E_F around these hole concentrations. This is consistent with the fact that the T_c of these doping levels show the highest T_c among the entire doping region.

As shown in Fig. 2, the overall features of the Fermi surfaces are in good agreement with the results of the LDA band-structure calculations.[19] However, according to the LDA calculation, the effects of k_z dependence are not negligible, particularly near the $(\pi,0)$ point for $x \geqslant 0.15$. Note that the ARPES results may detect spectra of particular k_z or an average of the spectra over k_z momentum because of the strong two dimensionality of LSCO. Therefore, the LDA dispersions around $(\pi,0)$ for different k_z's are plotted in Fig. 4. For $x=0.30$, the dispersion for $k_z=\pi/c$ best describes the experimental results as can be seen from Figs. 3(e) and 4(b), implying that the observed spectra were those of $k_z=\pi/c$ or the average over k_z. Alternatively, the k_z dispersion may have been suppressed by mass renormalization along the c axis. As shown in Fig. 4(a), there is small k_z dispersion on the $(\pi,0)$-(π,π) line in the LDA dispersions. Corresponding to this feature, for $x=0.03$, the k_F position of the underlying Fermi surface in the $(\pi,0)$-(π,π) direction almost coincides with that of the LDA result, although the spectral weight is strongly suppressed by the pseudogap opening. In the underdoped cuprates, the broad spectra around $(\pi,0)$ have been interpreted as a result of electron correlation effects. As shown in Fig. 4(a), the k_z dispersion may also cause additional broadening to the spectral features around $(\pi,0)$.

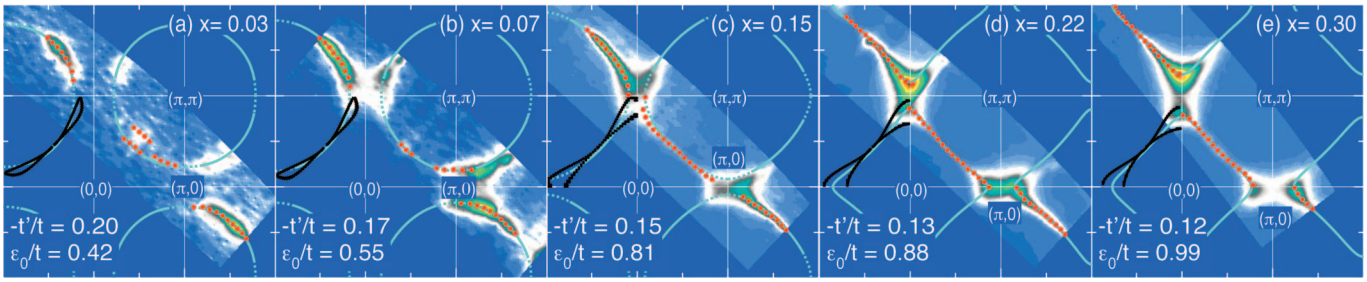

FIG. 2. (Color) Spectral weight map in k space at E_F in $La_{2-x}Sr_xCuO_4$. Red dots indicate k_F positions determined by the MDC peaks at E_F (see Fig. 1). The blue curves show the Fermi surface interpolated by the tight-binding model. The black curves are the Fermi surface for $k_z=0$ and $2\pi/c$ obtained from local-density-approximation (LDA) band-structure calculations (Ref. 19).

The experimental k_F's in Fig. 2 have been fitted to the 2D single-band tight-binding (TB) model $\varepsilon_k=\varepsilon_0-2t(\cos k_x a+\cos k_y a)-4t'\cos k_x a\cos k_y a-2t''(\cos 2k_x a+\cos 2k_y a)$, as shown by blue curves. Here, t, t', and t'' are the first-, second-, and third-nearest-neighbor transfer integrals between Cu sites. We have assumed constant $t=0.25$ eV and relationship $-t''/t'=1/2$ for all the doping levels, and regarded t' and ε_0 as adjustable parameters. The fitted results of the TB parameters, $-t'/t$ and ε_0/t, are shown in each panel of Fig. 2. Although the absolute values of t, t', and t'' are smaller than those determined by band-structure calculations by a factor of ~ 0.5, the relative magnitudes of the TB parameters agree rather well with the band-structure calculations—e. g., $-t'/t\sim 0.15$.[22] The Fermi surface is almost perfectly fitted by the TB model, although some misfit can be seen for the kink structure due to phonons (particulary in the nodal kink)[23,24] and the extremely flat band dispersion around $(\pi,0)$ in the underdoped region.

Here, the best-fit TB parameters $-t'/t$ indicated in Fig. 2 exhibit a clear increase with decreased doping, although residual k_z dispersion effects missing in this analysis should be kept in mind. The doping dependence of $-t'/t$ with decreasing x can be explained by the increase of the Cu–apical-oxygen distance with decreasing x (Ref. 25) according to LDA band-structure calculations for various single-layer cuprates.[22] When the distance becomes longer—i.e., the hybridization between the in-plane σ orbital (Cu $3d_{x^2-y^2}$ $+O2p_\sigma$) and the out-of-plane axial orbital (Cu $3d_{z^2}+O2p_z$ $+Cu4s$) becomes weaker, the $-t'/t$ becomes larger. Alternatively, the increase of $-t'/t$ with decreasing x is also consistent with the CDMFT calculation[9] and indicates the increasing correlation effects in the underdoped region. Note that the obtained parameters do not represent bare TB parameters but effective values influenced by the electron correlation.

B. Luttinger volume

Figure 5 summarizes the experimental Fermi surfaces. The intensity distributions clearly show an evolution of the pseudogap around $(\pi,0)$ and the shrinkage of the Fermi arc in the underdoped region. The underlying Fermi surfaces for each doping determined from the MDC analysis (Fig. 1) are shown in Fig. 5(f). The hole number deduced from the area of the experimental Fermi surface, x_{FS}, obtained assuming Luttinger's theorem, is plotted in Fig. 6(a) as a function of x. The plot of x_{FS} is seen to be located within the shaded region, which designates the limits of x_{FS} for different k_z values deduced from LDA (see black curves in Fig. 2),[19] implying that the observed x_{FS} may correspond to an averaged value over k_z. It is remarkable that x_{FS} is consistent with that predicted by Luttinger's theorem over the entire doping range. This result is in sharp contrast to that for Na-CCOC,[14] where x_{FS} deviates strongly from the predictions of the Luttinger's theorem in the underdoped region, as shown in Fig. 6(b). Interestingly, a closer inspection reveals that there is a tendency of deviation from Luttinger's theorem in the lightly doped LSCO ($x=0.03$) in the same direction as in Na-CCOC.

In order to highlight differences between the behaviors of the Fermi surfaces of LSCO and Na-CCOC, we have also plotted the doping dependence of the k_F value in the nodal direction in Fig. 6(b). Extrapolation of k_F to $x=0$ gives

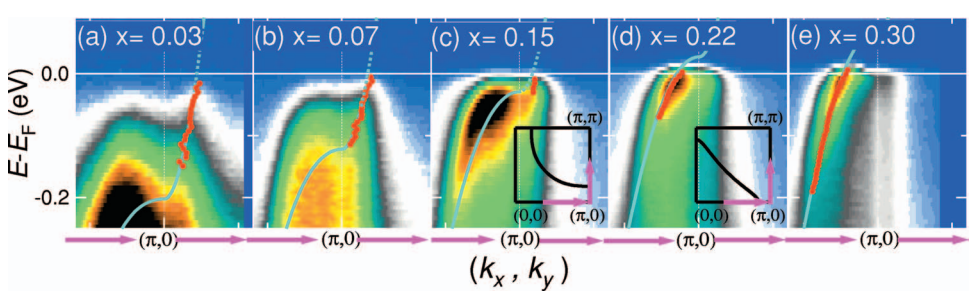

FIG. 3. (Color) Intensity plot in E-k space along the symmetry lines $(0,0)$-$(\pi,0)$-(π,π) in $La_{2-x}Sr_xCuO_4$. The direction and length of the arrows in the inset correspond to the horizontal axis of the color plots. Red dots indicate MDC peaks. The blue lines show the tight-binding interpolation.

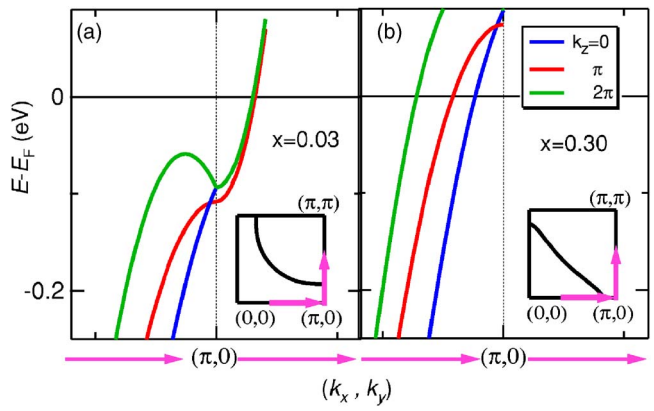

FIG. 4. (Color online) Energy dispersions for different k_z values (in units of $1/c$) obtained from the LDA band-structure calculations (Ref. 19).

$(\pi/2,\pi/2)$ for Na-CCOC, probably indicating that low-energy excitations in the low-doping limit come from (the tail of) the top of the lower Hubbard band (LHB), which has the band maximum at $(\pi/2,\pi/2)$ on the boundary of the antiferromagnetic BZ.[14,15] In contrast, the k_F in LSCO for $x=0.03$ is still away from $(\pi/2,\pi/2)$. This is related to the observation that the spectral weight at E_F comes from the QP peak which is well separated from the LHB.[13] While the LHB in Na-CCOC approaches E_F with hole doping,[15] that in LSCO stays away from E_F even as the spectral weight is transferred to the QP band near E_F.[13] This difference between LSCO and Na-CCOC is also reflected in different chemical potential shifts in the two cases; i.e., while photoemission spectra of Na-CCOC show rigid shifts with hole doping,[15] those of LSCO show slow shifts reflecting pinning of the chemical potential at the in-gap states.[26] Although a large Fermi surface is observed in Na-CCOC, the doping evolution of the electronic structure is somewhat similar to the small Fermi-surface picture in the sense that the chemical potential appears to be shifted downwards from the top of

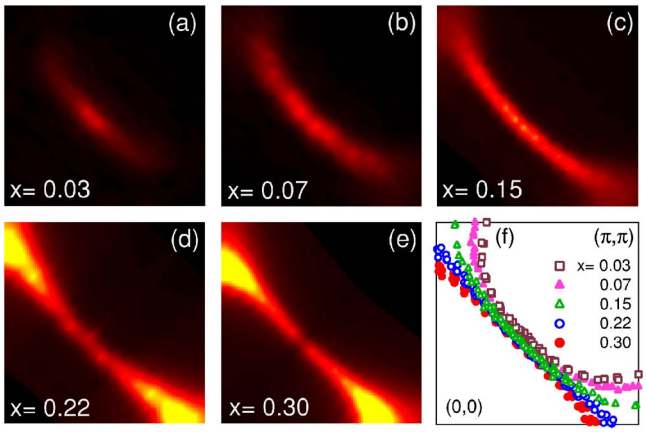

FIG. 5. (Color online) Doping dependence of the underlying Fermi surface in $La_{2-x}Sr_xCuO_4$. (a)–(e) Spectral weight mapping in k space at E_F. The intensities in the second BZ of Fig. 2 have been symmetrized with respect to the node direction. (f) k_F position for each doping determined by extrapolating MDC peaks to E_F.

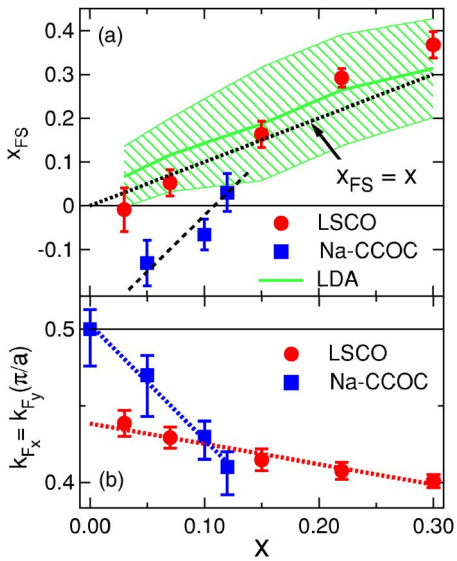

FIG. 6. (Color online) (a) Doping dependence of the hole number x_{FS} deduced from the Fermi surface area. Luttinger's theorem $x_{FS}=x$ is shown for comparison. The shaded region indicates the range of x_{FS} due to k_z variation deduced from LDA band-structure calculations (Ref. 19); the green line gives the average of the shaded region. (b) Doping dependence of the k_F value in the nodal direction. Data for Na-CCOC (Ref. 14) are also plotted. Dashed lines in (a) and (b) are guides to the eye.

the LHB. In a recent theoretical study, the nature of the small Fermi surface has been discussed as an origin of the apparent disagreement with Luttinger's theorem.[17]

Recently, the LHB's in underdoped La_2CuO_4 and $Ca_2CuO_2Cl_2$ have been interpreted as polaronic sidebands.[15,27] While this picture explains well the LHB feature of the undoped samples, it does not straightforwardly explain the aforementioned differences between the doping evolution of LSCO and Na-CCOC. In the polaronic picture, the peak of the LHB is shifted towards the E_F with hole doping since electron-phonon coupling is weakened by screening effects. However, the peak of the LHB in LSCO stays almost at the same binding energy with hole doping in the underdoped regime. This suggests that in LSCO the local charge density does not change with hole doping, reminiscent of a phase separation between the hole-poor and hole-rich regions. Indeed, the chemical potential pinning observed in LSCO (Ref. 26) would be a natural consequence of the presence of a mixture of different hole concentrations.

According to a recent theoretical study, a mixed phase of antiferromagnetic (AF) and superconducting (SC) states is proposed to explain the coexistence of the QP states and the LHB in LSCO,[28] and captures the characteristic two-component behavior of the ARPES results of underdoped LSCO.[13,29] This picture has been corroborated by a recent transport study in lightly doped LSCO.[30] Also, it has been predicted that phase separation between the insulating and metallic phases occurs under a certain regime of electron-phonon coupling strengths.[31] For a macroscopically phase-separated state, one would normally expect to observe two Fermi surfaces corresponding to the two phases. If there are sufficiently fast dynamical fluctuations between the two

phases, however, one might see only an average Fermi surface roughly obeying the Luttinger's theorem.

IV. SUMMARY

In the present study, we have observed systematic changes in the underlying Fermi surfaces in LSCO over a wide doping range. The area of the Fermi surface so obtained approximately satisfies Luttinger's theorem even in the lightly doped region. This behavior is contrasted with that of Na-CCOC, which shows a clear deviation from Luttinger's theorem. Possible origins of the differences between LSCO and Na-CCOC are discussed in relation to the chemical potential pinning and possible phase separation in underdoped LSCO.

ACKNOWLEDGMENTS

We are grateful to P. Prelovsek, N. Nagaosa, C. M. Ho, and M. Ido for enlightening discussions. This work was supported by a Grant-in-Aid for Scientific Research in Priority Area "Invention of Anomalous Quantum Materials," Grant-in-Aid for Young Scientists from the Ministry of Education, Science, Culture, Sports and Technology, and the U.S. DOE Contracts No. DE-FG03-01ER45876 and No. DE-AC03-76SF00098, and benefited from the allocation of supercomputer time at NERSC and Northeastern University's Advanced Scientific Computation Center (ASCC). ALS is operated by the Department of Energy's Office of Basic Energy Science, Division of Materials Science.

[1] A. Damascelli, Z. Hussain, and Z.-X. Shen, Rev. Mod. Phys. **75**, 473 (2003).
[2] J. W. Loram, K. A. Mirza, J. M. Wade, J. R. Cooper, and W. Y. Liang, Physica C **235–240**, 134 (1994).
[3] N. Momono, T. Matsuzaki, M. Oda, and M. Ido, J. Phys. Soc. Jpn. **71**, 2832 (2002).
[4] T. Nakano, M. Oda, C. Manabe, N. Momono, Y. Miura, and M. Ido, Phys. Rev. B **49**, 16000 (1994).
[5] S. Chakravarty, R. B. Laughlin, D. K. Morr, and C. Nayak, Phys. Rev. B **63**, 094503 (2001).
[6] M. E. Simon and C. M. Varma, Phys. Rev. Lett. **89**, 247003 (2002).
[7] P. Prelovsek and A. Ramsak, Phys. Rev. B **65**, 174529 (2002).
[8] H. Fukuyama and H. Kohno, in *Physics and Chemistry of Transition-Metal Oxides*, edited by H. Fukuyama and N. Nagaosa (Springer, Berlin, 1999), p. 231.
[9] M. Civelli, M. Capone, S. S. Kancharla, O. Parcollet, and G. Kotliar, Phys. Rev. Lett. **95**, 106402 (2005).
[10] G. Esirgen, H.-B. Schüttler, C. Gröber, and H. G. Evertz, Phys. Rev. B **64**, 195105 (2001).
[11] T. A. Maier, T. Pruschke, and M. Jarrell, Phys. Rev. B **66**, 075102 (2002).
[12] W. O. Putikka, M. U. Luchini, and R. R. P. Singh, Phys. Rev. Lett. **81**, 2966 (1998).
[13] T. Yoshida, X. J. Zhou, T. Sasagawa, W. L. Yang, P. V. Bogdanov, A. Lanzara, Z. Hussain, T. Mizokawa, A. Fujimori, H. Eisaki, Z.-X. Shen, T. Kakeshita, and S. Uchida, Phys. Rev. Lett. **91**, 027001 (2003).
[14] K. M. Shen, F. Ronning, D. H. Lu, F. Baumberger, N. J. C. Ingle, W. S. Lee, W. Meevasana, Y. Kohsaka, M. Azuma, M. Takano, H. Takagi, and Z.-X. Shen, Science **307**, 901 (2005).
[15] K. M. Shen, F. Ronning, D. H. Lu, W. S. Lee, N. J. C. Ingle, W. Meevasana, F. Baumberger, A. Damascelli, N. P. Armitage, L. L. Miller, Y. Kohsaka, M. Azuma, M. Takano, H. Takagi, and Z.-X. Shen, Phys. Rev. Lett. **93**, 267002 (2004).
[16] Y. Ando, A. N. Lavrov, S. Komiya, K. Segawa, and X. F. Sun, Phys. Rev. Lett. **87**, 017001 (2001).
[17] K. Y. Yang, T. M. Rice, and F. C. Zhang, Phys. Rev. B **73**, 174501 (2006).
[18] R. Sensarma, M. Randeria, and N. Trivedi, cond-mat/0607006 (unpublished).
[19] S. Sahrakorpi, M. Lindroos, R. S. Markiewicz, and A. Bansil, Phys. Rev. Lett. **95**, 157601 (2005).
[20] T. Yoshida, X. J. Zhou, M. Nakamura, S. A. Kellar, P. V. Bogdanov, E. D. Lu, A. Lanzara, Z. Hussain, A. Ino, T. Mizokawa, A. Fujimori, H. Eisaki, C. Kim, Z.-X. Shen, T. Kakeshita, and S. Uchida, Phys. Rev. B **63**, 220501(R) (2001).
[21] The origin of the "shadow band" is discussed in A. Koitzsch *et al.*, Phys. Rev. B **69**, 220505(R) (2004), in terms of structual effects.
[22] E. Pavarini, I. Dasgupta, T. Saha-Dasgupta, O. Jepsen, and O. K. Andersen, Phys. Rev. Lett. **87**, 047003 (2001).
[23] A. Lanzara, P. V. Bogdanov, X. J. Zhou, S. A. Kellar, D. L. Feng, E. D. Lu, T. Yoshida, H. Eisaki, A. Fujimori, K. Kishio, J.-I. Shimoyama, T. Noda, S. Uchida, Z. Hussain, and Z.-X. Shen, Nature (London) **412**, 510 (2001).
[24] X. J. Zhou *et al.*, Nature (London) **423**, 398 (2003).
[25] P. G. Radaelli, D. G. Hinks, A. W. Mitchell, B. A. Hunter, J. L. Wagner, B. Dabrowski, K. G. Vandervoort, H. K. Viswanathan, and J. D. Jorgensen, Phys. Rev. B **49**, 4163 (1994).
[26] A. Ino, T. Mizokawa, A. Fujimori, K. Tamasaku, H. Eisaki, S. Uchida, T. Kimura, T. Sasagawa, and K. Kishio, Phys. Rev. Lett. **79**, 2101 (1997).
[27] O. Rösch, O. Gunnarsson, X. J. Zhou, T. Yoshida, T. Sasagawa, A. Fujimori, Z. Hussain, Z.-X. Shen, and S. Uchida, Phys. Rev. Lett. **95**, 227002 (2005).
[28] M. Mayr, G. Alvarez, A. Moreo, and E. Dagotto, Phys. Rev. B **73**, 014509 (2006).
[29] A. Ino, C. Kim, M. Nakamura, T. Yoshida, T. Mizokawa, Z.-X. Shen, A. Fujimori, T. Kakeshita, H. Eisaki, and S. Uchida, Phys. Rev. B **62**, 4137 (2000).
[30] Y. Ando, A. N. Lavrov, and S. Komiya, Phys. Rev. Lett. **90**, 247003 (2003).
[31] M. Capone, G. Sangiovanni, C. Castellani, C. Di Castro, and M. Grilli, Phys. Rev. Lett. **92**, 106401 (2004).